Letter

Simple predictors of T_c in superconducting cuprates and the role of interactions between effective Wannier orbitals in the d-p three-band model

Jakša Vučičević [1] and Michel Ferrero [2,3]

[1]*Scientific Computing Laboratory, Center for the Study of Complex Systems, Institute of Physics Belgrade, University of Belgrade, Pregrevica 118, 11080 Belgrade, Serbia*

[2]*CPHT, CNRS, Ecole Polytechnique, Institut Polytechnique de Paris, Route de Saclay, 91128 Palaiseau, France*

[3]*Collège de France, 11 place Marcelin Berthelot, 75005 Paris, France*

(Received 18 August 2023; revised 12 December 2023; accepted 1 February 2024; published 26 February 2024)

At optimal doping, different cuprate compounds can exhibit vastly different critical temperatures for superconductivity (T_c), ranging from about 20 to about 135 K. The precise properties of the lattice that determine the magnitude of the T_c are currently unknown. In this paper, we investigate the dependence of the optimal doping T_c on the parameters of the Emery (d-p) model for the CuO_2 planes in the cuprates. We show that the best scaling is obtained not with the parameters of the model written in the real (d/p-orbital) space but rather written in the space of effective Wannier orbitals. In this basis, one obtains a model of three sublattices coupled through all possible four-point interactions. We identify multiple predictor variables that fit the experimental T_c to about $\pm$4–5 K and that remarkably depend on the leading attractive coupling constants in the transformed Hamiltonian.

DOI: 10.1103/PhysRevB.109.L081115

Finding ways to increase the superconducting critical temperature in cuprate compounds is one of the central goals in condensed matter physics [1–4]. The record T_c remains at about 135 K for already more than two decades [5,6] (if we only consider systems at atmospheric pressure [7,8]). One of the reasons for the lack of progress is that there is no clear understanding of what to look for in a crystal structure, if one is to identify a high-T_c candidate. Many works focused on how T_c correlates with the tight-binding parameters [9–26]. The role of phonons [27–31] and disorder [32–34] have been considered as well. In more recent machine learning approaches [35–38], a large number of different quantities was considered systematically. Even though the Coulomb interaction is widely believed to be responsible for superconductivity in the cuprates, no works to our knowledge have attempted to systematically link *ab initio* computed coupling constants to the experimentally measured T_c for multiple compounds.

Studies so far have mostly looked at correlations between the T_c and the parameters of two kinds of models: single-band and three-band. In the single-band picture, the main idea was that longer range hopping (t') frustrates the antiferromagnetic (AFM) correlations, which are believed to act as the pairing glue in the cuprates [22,39–44]. However, the experimentally observed trend in $T_c(t'/t)$ [11,13,18] was not reproduced in single-band calculations [12,14,16,19,24–26,45], thus suggesting that the single-band models (both Hubbard and $tt'J$) do not capture all the mechanisms that determine the T_c in the cuprates. In the three-band d-p (Emery) model picture, some works considered the charge-transfer gap (CTG, the difference in energy between copper d and oxygen p orbitals [18,44,46], or defined by the gap in the local spectral function [44,47]) as the relevant energy scale that determines the strength of the effective AFM coupling, and thus the T_c. At least some trends of how the experimental T_c depends on the tight-binding parameters computed for the Emery model can be reproduced by many-body calculations (see Ref. [18] and compare to Ref. [15]). More recently, experimentally observed trends of how T_c depends on the density of holes on the copper and oxygen sites separately [48] was also reproduced in calculations for the d-p model [47]. These findings seem to indicate that the Emery model is more relevant for the description of the T_c magnitude in the cuprates. However, the attempt [18] to quantitatively correlate the tight-binding parameters of the Emery model to the experimentally measured T_c yielded only poor fits, with large standard deviation of about 30 K. This still leaves open the question of the practical relevance of the CTG and the Emery model.

In this paper, we show that the experimentally measured T_c can indeed be described by a simple function of three Emery-model tight-binding parameters (computed for each compound using *ab initio* methods), with a small standard deviation of about 7 K. Furthermore, we show that the interplay between interaction and geometry plays an essential role, and that even better fits can be obtained if one considers not only the tight-binding parameters, but also the coupling constants. The effective onsite repulsion on copper sites U_{dd} is unlikely to depend strongly on the specifics of the lattice structure; However, if one transforms the Hamiltonian in such a way that the e-e coupling and the kinetic energy become entangled, the resulting coupling constants can be strongly material dependent. By using one such (exact) transformation, we formally obtain a model of three separate square lattices, coupled through all possible four-point interactions between two electrons. Among the coupling constants, some are positive (repulsive), and some are negative (attractive). We find that the experimentally measured T_c can be fit to within about 5 K, by using a linear function of only two parameters of our transformed Hamiltonian, one of them being the leading attractive interaction. We explore the correlations of T_c with the parameters of our transformed model in a systematic and

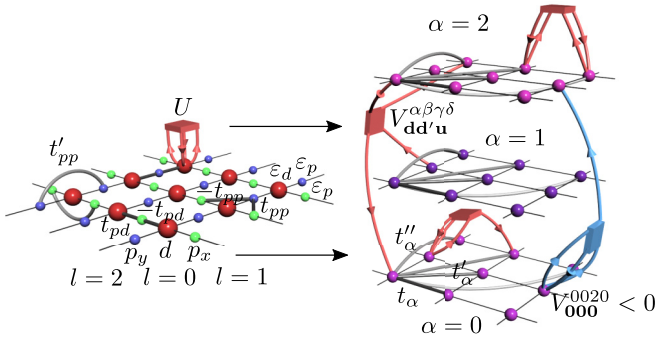

FIG. 1. Illustration of the Hamiltonian transformation. A lattice model of d and p orbitals with only local density-density interactions on the d orbitals is exactly transformed into a model of three square lattices with longer range hoppings and a zoo of four-point interactions, some of which are attractive.

unbiased way. Our results indicate the presence of additional pairing (or pair-breaking) mechanisms in the cuprates, which might strongly affect the magnitude of T_c. These mechanisms do not have a simple interpretation in terms of the d and p orbitals, but are apparently related to density-assisted hopping processes between certain spatially extended states, as captured by the Hamiltonian terms in our transformed model. This is particularly interesting in the view of the recent publication of *Jiang et al.* [49] which showed in a many-body calculation that such coupling terms can indeed strongly affect the T_c.

Model. The Emery model [18,47,50] (illustrated on Fig. 1) has a unit cell that contains a copper d orbital and two oxygen p orbitals (denoted with $l = 0, 1, 2 \equiv d, p_x, p_y$). The d orbitals form a square lattice, and the p orbitals are found in between the neighboring d orbitals. The hopping amplitude between d and p orbitals is $\pm t_{pd}$, depending on the direction, and, similarly, between the p_x and p_y orbitals the hopping amplitude is $\pm t_{pp}$. The hopping between the nearest p_x (p_y) orbitals is t'_{pp}.

The noninteracting part of the Hamiltonian can be diagonalized by switching to the basis of appropriate Bloch waves $d^\dagger_{\alpha,\sigma,\mathbf{k}}|0\rangle$ (see Ref. [51])

$$\hat{H}_0 = \sum_{\sigma,\alpha,\mathbf{k}} E_{\alpha,\mathbf{k}} d^\dagger_{\alpha,\sigma,\mathbf{k}} d_{\alpha,\sigma,\mathbf{k}}, \tag{1}$$

where $\alpha = 0, 1, 2$ enumerates the eigenbands in the order of ascending energy, and $\mathbf{k}$ is a wave-vector in the first Brillouin zone. The spin projection $(\uparrow, \downarrow)$ is denoted σ.

In terms of the original local orbitals (denoted l), the interacting part of the Hamiltonian, as considered in Refs. [18,47] can be written in two spin-symmetric ways

$$\hat{H}_{\text{int}} = \frac{1}{2}\sum_{l,\sigma,\mathbf{r}} U_l c^\dagger_{l,\sigma,\mathbf{r}} c_{l,\sigma,\mathbf{r}} c^\dagger_{l,\bar{\sigma},\mathbf{r}} c_{l,\bar{\sigma},\mathbf{r}} \tag{2}$$

$$= \frac{1}{2}\sum_{l,\sigma\sigma',\mathbf{r}} U_l c^\dagger_{l,\sigma,\mathbf{r}} c_{l,\sigma,\mathbf{r}} c^\dagger_{l,\sigma',\mathbf{r}} c_{l,\sigma',\mathbf{r}} - \sum_{l,\sigma,\mathbf{r}} \frac{U_l}{2} c^\dagger_{l,\sigma,\mathbf{r}} c_{l,\sigma,\mathbf{r}} \tag{3}$$

with $U_l = U\delta_{l,0}$, and $\bar{\sigma}$ denotes the spin projection opposite of σ. The real-space position of the unit cell is denoted $\mathbf{r}$. The expressions (2) and (3) are equivalent. However, the choice of one or the other will make a difference for the final form of the Hamiltonian that we reach, following our (exact) transformation: the values of the constants in front of different Hamiltonian terms that we obtain, as well as their physical meaning, will depend on how we initially formulate the interacting part. The quadratic term in Eq. (3) will be absorbed in the noninteracting part, and will amount to a shift $\varepsilon_d \to \varepsilon_d - U/2$. More importantly, only the choice Eq. (3) will yield a formulation with a spin-rotational symmetry. We will refer to the formulation based on Eq. (2) [Eq. (3)] as model A (model B).

We now rewrite the entire Hamiltonian in the eigenbasis of the noninteracting part and then further perform the (inverse) Fourier transformation: we express the Hamiltonian in terms of the operators $d^\dagger_{\alpha,\sigma,\mathbf{r}} = \frac{1}{\sqrt{N}}\sum_{\mathbf{k}} e^{-i\mathbf{k}\cdot\mathbf{r}} d^\dagger_{\alpha,\sigma,\mathbf{k}}$. There is a phase ambiguity associated with the definition of the operators $d^\dagger_{\alpha,\sigma,\mathbf{k}}$ [52] which we discuss in more detail in Ref. [51]. The choice of the phase we make ensures that, in the final form of the Hamiltonian, all hopping amplitudes and coupling constants are purely real and are consistent with the symmetries of the original lattice. We obtain

$$\hat{H} = \sum_{\sigma,\alpha,\mathbf{rd}} t_{\alpha,\mathbf{d}} d^\dagger_{\alpha,\sigma,\mathbf{r}} d_{\alpha,\sigma,\mathbf{r}+\mathbf{d}} + \frac{1}{2}\sum_{\substack{\sigma\sigma',\alpha\beta\gamma\delta \\ \mathbf{rdd'u}}} V^{\alpha\beta\gamma\delta}_{\mathbf{dd'u}} d^\dagger_{\alpha,\sigma,\mathbf{r}} d_{\beta,\sigma,\mathbf{r}+\mathbf{d}} d^\dagger_{\gamma,\sigma',\mathbf{r}+\mathbf{u}-\mathbf{d'}} d_{\delta,\sigma',\mathbf{r}+\mathbf{u}}, \tag{4}$$

where $t_{\alpha,\mathbf{d}}$ is the inverse Fourier transform of $E_{\alpha,\mathbf{k}}$, and it has full square-lattice symmetry. For the precise definition of the coupling constants $V^{\alpha\beta\gamma\delta}_{\mathbf{dd'u}}$ see Ref. [51].

The transition from Eqs. (1) and (3) to Eq. (4) is exact, and is illustrated in Fig. 1. Starting from Eqs. (1) and (2) instead, the only formal difference is the absence of the $\sigma = \sigma'$ terms in the interacting part in Eq. (4), but $t_{\alpha,\mathbf{d}}$ and $V^{\alpha\beta\gamma\delta}_{\mathbf{dd'u}}$ values will also be different (due to the absence of the shift $\varepsilon_d \to \varepsilon_d - U/2$).

Dataset. We revisit the dataset compiled by *Weber et al.* [18,53], where Emery model parameters were evaluated from density functional theory (DFT) band-structures for 16 different cuprates (stoichiometric, parent compounds). For two three-layer compounds, parameters were computed separately for the inner and outer layers, which makes the total number of data points in the dataset 18. The data includes the four parameters of the quadratic part of the Hamiltonian written in real-space (onsite energies and hopping amplitudes), as well as the ratio of the next-nearest and the nearest neighbor hoppings t'/t in an effective single-band model that *Weber et al.* derived based on the d-p model parameters. The density-density interaction was only assumed to exist on the d-orbitals, and was considered to be the same for all compounds, 8 eV.

Weber et al. only fitted T_c to individual model parameters. The fits were rather poor [see Ref. [51] and Fig. 2(a)]. The T_c was found to correlate with $\varepsilon_d - \varepsilon_p$ (the CTG) in the expected

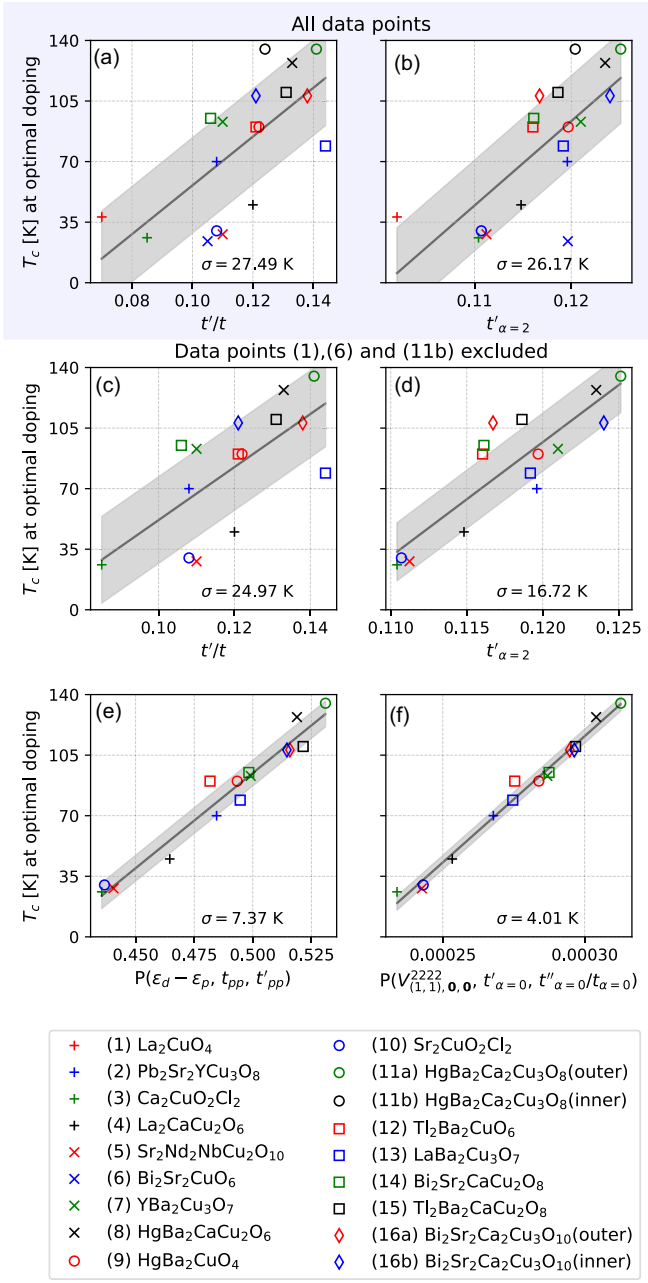

FIG. 2. Test of different predictors of T_c. The standard deviation of each fit is denoted σ. The black line is the linear fit, the width of the gray shading corresponds to $\pm\sigma$.

way, but only weakly. In our opinion, one should not expect that a single Hamiltonian term controls the T_c in its entirety. One should rather expect a competition (or cooperation) between different processes encoded in the Hamiltonian. Most generally, if the Emery model is correct for the cuprates, the T_c should in general be a single-valued function of *all* the parameters, $T_c(\varepsilon_d - \varepsilon_p, t_{pd}, t_{pp}, t'_{pp})$. This was not checked in *Weber et al.*, and based on their analyses, one cannot give a clear assessment of the relevance of the Emery model for the cuprates. We provide such a check on Fig. 2(e) (see also Ref. [51]). We demonstrate that a linear combination of three of the Emery model parameters, namely $\epsilon_d - \epsilon_p$, t_{pp}, and t'_{pp} is a solid predictor of T_c, to within ± 7.4 K in the whole range of T_c, except for three apparent outliers (see the explanations in the next section). The remaining variance of our fit could be attributed to t_{pd}, but we find that adding this parameter to the linear combination does not bring much improvement: T_c is not a linear function of t_{pd}. The remaining variance could also be due to parameters not included in the Emery model. However, T_c does fit linearly and with an even smaller standard deviation to the parameters of our transformed Hamiltonian, as we show in the following: this presents strong evidence that the Emery model indeed captures the mechanisms that dominantly determine the T_c.

Strategy and results. For each entry in the *Weber et al.* dataset (given in Ref. [51]), we evaluate the dispersions and *all* the parameters of the Hamiltonian in Eq. (4). We then compute from these values about 50 variables that we expect might correlate with T_c (these include the bandwidths of each band D_α, short-distance hoppings $t_\alpha \equiv t_{\alpha,\mathbf{d}=(1,0)}$, $t'_\alpha \equiv t_{\alpha,\mathbf{d}=(1,1)}$, $t''_\alpha \equiv t_{\alpha,\mathbf{d}=(2,0)}$, as well as various short-distance components and extremal values of $V^{\alpha\beta\gamma\delta}_{\mathbf{dd'u}}$).

We first look at the correlation with the T_c of each individual variable, by doing a linear fit and estimating the standard deviation, σ. We find that the best predictor is $t'_{\alpha=2}$ (in model B formulation), yielding a fit with $\sigma = 26.2$ K. This is slightly better than the t'/t for the effective single band put forward by *Weber et al.*, but t'/t is, indeed, a close second with $\sigma = 27.5$ K (see Fig. 2 top row). We readily see that the data points (1), (6), and (11b) are outliers for both of the best predictors. In our other attempts at fitting the T_c, these three points were consistently presenting a limiting factor in obtaining a small σ. Both points (1) and (6) have a very low T_c—the point (6) has even the lowest T_c (it was also found to be an outlier in Ref. [9]), while the point (1) is extreme in terms of many of the model parameters, so we exclude both points from further analysis. The point (11b) represents the parameters for the inner layer of a three-layer material, and it may be that the outer layer paramaters, given by the data point (11a), are more relevant, so we exclude the point (11b), as well. In total, we are left with 15 data points, for 14 different compounds. We then redo the fits with respect to individual parameters, and we see that σ for the t'/t fit has dropped to about 25 K, while the σ for the $t'_{\alpha=2}$ fit has dropped to 16.7 K. In our subset of data which excludes the apparent outliers, $t'_{\alpha=2}$ is by far the best single-parameter predictor of T_c. This holds even in the case of model A.

We now construct all possible linear combinations of any two and three variables, $P(p_1, p_2[, p_3]) = c_1 p_1 + c_2 p_2[+c_3 p_3]$, and we keep fixed $\sum_i c_i^2 = 1$. For each of the ~1200 pairs (p_1, p_2) and ~40 000 triplets (p_1, p_2, p_3), we pinpoint the minimum in $\sigma(\{p_i\};\{c_i\})$ using the Nelder-Mead algorithm. We then rank different pairs and triplets according to the minimum standard deviation that we can obtain, $\min_{\{c_i\}} \sigma(\{p_i\};\{c_i\})$. Finally, we count the number of times each variable appears in the top 100 triplets, to gain insight into which parameters might be most relevant. Our results are summarized in Table I (see also Ref. [51]).

We observe a general trend in our results, regardless of the choice of the formulation of the interaction part [Eq. (2) or (3)]—good predictors are the linear combinations of a

TABLE I. Summary of the best predictors of T_c. In the first column, we restrict to only the original 4 parameters of the model and the t'/t for the effective single-band model computed in *Weber et al.* In the second and third columns, we include the parameters of models A and B, respectively, and variables computed from those parameters.

category	Original parameters and t'/t	σ (K)	Model A	σ (K)	Model B	σ (K)
one-param. best	t'/t	24.97	$t'_{\alpha=2}$	21.70	$t'_{\alpha=2}$	16.72
two-param. best	$\varepsilon_d - \varepsilon_p, t_{pp}$	12.67	$t''_{\alpha=1}, \min V^{\alpha\beta\gamma\delta}_{\mathbf{dd'u}}$	5.42	$t'_{\alpha=1}, V^{0000}_{(1,1),(-1,-1),\mathbf{0}}$	5.74
three-param. best	$\varepsilon_d - \varepsilon_p, t_{pp}, t'_{pp}$	7.37	$D_{\alpha=1}, t''_{\alpha=1}, t'_{\alpha=2}$	4.47	$t'_{\alpha=0}, \frac{t''_{\alpha=0}}{t_{\alpha=0}}, V^{2222}_{(1,1),\mathbf{0},\mathbf{0}}$	4.01
tree-param. second best	$\varepsilon_d - \varepsilon_p, t_{pp}, t'/t$	9.74	$D_{\alpha=1}, t''_{\alpha=1}, V^{2222}_{\mathbf{0},\mathbf{0},\mathbf{0}}$	4.55	$t'_{\alpha=0}, \min V^{0000}_{\mathbf{dd'u}}, V^{2222}_{(1,1),\mathbf{0},\mathbf{0}}$	4.03

hopping amplitude and one or two coupling constants, in many cases the attractive ones, and in most cases those acting within or between the bands $\alpha = 0$ and 2, which are precisely the bands having an appreciable amount of d character.

The best two-parameter predictor we find is the linear combination of the overall most attractive component of $V^{\alpha\beta\gamma\delta}_{\mathbf{dd'u}}$ and the hopping amplitude $t''_{\alpha=1}$ (obtained in the model A formulation), yielding $\sigma = 5.4$ K. The most attractive component in both model A and B formulations is the local density-assisted hybridization from band $\alpha = 0$ to band $\alpha = 2$, $V^{0020}_{\mathbf{0},\mathbf{0},\mathbf{0}}$.

The best result that we have obtained in our unbiased search is given in Fig. 2(f). A linear combination of $V^{2222}_{(1,1),\mathbf{0},\mathbf{0}}$, $t'_{\alpha=0}$ and $t''_{\alpha=0}/t_{\alpha=0}$, obtained in model B, yields a fit of T_c with $\sigma = 4.01$ K. The coupling constant $V^{2222}_{(1,1),\mathbf{0},\mathbf{0}}$ is negative and corresponds to an assisted hopping term in the $\alpha = 2$ band, say $n_{\alpha,\uparrow,\mathbf{r}} d^\dagger_{\alpha,\downarrow,\mathbf{r}} d_{\alpha,\downarrow,\mathbf{r}+(1,1)}$ (similar to the terms considered in *Jiang et al.*). The parameters $V^{2222}_{(1,1),\mathbf{0},\mathbf{0}}$, $t'_{\alpha=0}$ appear the most times in the top 100 three-parameter predictors based on model B, in total 65 times. It is interesting that $t''_{\alpha=0}/t_{\alpha=0}$ correlates closely with $V^{0000}_{(2,0),\mathbf{0},\mathbf{0}}$, which is, at the same time, the most attractive interaction in the $\alpha = 0$ band. Indeed, the linear combination of $V^{2222}_{(1,1),\mathbf{0},\mathbf{0}}$, $t'_{\alpha=0}$ and $\min V^{0000}_{\mathbf{dd'u}}$ is our close second best result, with $\sigma = 4.03$.

Finally, we find that the local density-density interaction in the $\alpha = 2$ band, $V^{2222}_{\mathbf{000}}$, might be very relevant. In model A, it appears the most times in the top 100 three-parameter predictors, and in model B it is in this sense ranked sixth. In all linear combinations in which it appears, $V^{2222}_{\mathbf{000}}$ enters with a negative coefficient. Intuitively, a weaker local repulsion could mean a higher T_c. The best single-parameter predictor, $t'_{\alpha=2}$, indeed, highly (anti)correlates with $V^{2222}_{\mathbf{000}}$ (see Table I and Ref. [51] for details).

Discussion and prospects for future work. Our results provide strong evidence that the Emery model well captures the mechanisms that determine the magnitude of T_c in the cuprates. We identify multiple terms in the Hamiltonian which appear particularly relevant for the T_c, and propose that these correspond to additional pairing and pair-breaking mechanisms that are in competition. These processes can be understood only in terms of the spatially extended, effective Wannier orbitals in the Emery model, which were not considered in earlier works.

In addition, we obtain a large set of predictor variables that can be computed cheaply, and thus used practically in high-throughput [54–56] searches for novel high-T_c candidate structures. For practical use, the main question is whether the simple relation between T_c and our predictor variables holds outside the region of the parameter-space that is covered by the *Weber et al.* data points. The best strategy is then to look at crystal structures inside or close to that region, and focus on points for which multiple predictors agree. We have scanned the parameter space, and we find a case where each of the four parameters of the Emery model is inside the range of values for the existing cuprates, and for which our top 100 predictor variables (based on model B) predict $T_c \approx 195 \pm 5$ K. Going only slightly away from the range of Emery model parameters covered by the data points, we find cases which correspond to T_c of even more than 250 K (see Ref. [51] for details).

As was the case with previous similar works, the main limitation of our approach lies in the ambiguity of the DFT calculations [57,58] and the downfolding procedures [49,59], especially when it comes to the choice and computation of Coulomb tensor elements; our work ultimately highlights the necessity of a careful and systematic work in that direction.

Acknowledgments. We acknowledge useful discussions with A.-M. S. Tremblay and Antoine Georges. We acknowledge contributions from Bogdan Rajkov and Sidhartha Dash in the early stages of this work. Computations were performed on the PARADOX supercomputing facility (Scientific Computing Laboratory, Center for the Study of Complex Systems, Institute of Physics Belgrade). J.V. acknowledges funding provided by the Institute of Physics Belgrade, through the grant by the Ministry of Science, Technological Development and Innovation of the Republic of Serbia. J.V. acknowledges funding by the European Research Council, Grant No. ERC-2022-StG: 101076100.

[1] A. P. Malozemoff, J. Mannhart, and D. Scalapino, High-temperature cuprate superconductors get to work, Phys. Today **58**, 41 (2005).

[2] P. A. Lee, N. Nagaosa, and X.-G. Wen, Doping a mott insulator: Physics of high-temperature superconductivity, Rev. Mod. Phys. **78**, 17 (2006).

[3] Z. Guven Ozdemir, O. Aslan Cataltepe, and U. Onbasli, Some contemporary and prospective applications of high temperature superconductors, in *Applications of High-Tc Superconductivity*, edited by A. Moysés Luiz (InTech, Rijeka, Croatia, 2011).

[4] M. R. Norman, The challenge of unconventional superconductivity, Science **332**, 196 (2011).

[5] A. Schilling, M. Cantoni, J. D. Guo, and H. R. Ott, Superconductivity above 130 K in the Hg-Ba-Ca-Cu-O system, Nature (London) **363**, 56 (1993).

[6] B. Keimer, S. A. Kivelson, M. R. Norman, S. Uchida, and J. Zaanen, From quantum matter to high-temperature superconductivity in copper oxides, Nature (London) **518**, 179 (2015).

[7] I. A. Troyan, D. V. Semenok, A. G. Ivanova, A. G. Kvashnin, D. Zhou, A. V. Sadakov, O. A. Sobolevsky, V. M. Pudalov, I. S. Lyubutin, and A. R. Oganov, High-temperature superconductivity in hydrides, Phys. Usp. **65**, 748 (2022).

[8] A. P. Drozdov, M. I. Eremets, I. A. Troyan, V. Ksenofontov, and S. I. Shylin, Conventional superconductivity at 203 Kelvin at high pressures in the sulfur hydride system, Nature (London) **525**, 73 (2015).

[9] Y. Ohta, T. Tohyama, and S. Maekawa, Apex oxygen and critical temperature in copper oxide superconductors: Universal correlation with the stability of local singlets, Phys. Rev. B **43**, 2968 (1991).

[10] L. F. Feiner, M. Grilli, and C. Di Castro, Apical oxygen ions and the electronic structure of the high-T_c cuprates, Phys. Rev. B **45**, 10647 (1992).

[11] R. Raimondi, J. H. Jefferson, and L. F. Feiner, Effective single-band models for the high-T_c cuprates. II. role of apical oxygen, Phys. Rev. B **53**, 8774 (1996).

[12] Th. Maier, M. Jarrell, Th. Pruschke, and J. Keller, d-wave superconductivity in the Hubbard model, Phys. Rev. Lett. **85**, 1524 (2000).

[13] E. Pavarini, I. Dasgupta, T. Saha-Dasgupta, O. Jepsen, and O. K. Andersen, Band-structure trend in hole-doped cuprates and correlation with $T_{c\,\max}$, Phys. Rev. Lett. **87**, 047003 (2001).

[14] S. R. Hassan, B. Davoudi, B. Kyung, and A.-M. S. Tremblay, Conditions for magnetically induced singlet d-wave superconductivity on the square lattice, Phys. Rev. B **77**, 094501 (2008).

[15] P. R. C. Kent, T. Saha-Dasgupta, O. Jepsen, O. K. Andersen, A. Macridin, T. A. Maier, M. Jarrell, and T. C. Schulthess, Combined density functional and dynamical cluster quantum Monte Carlo calculations of the three-band Hubbard model for hole-doped cuprate superconductors, Phys. Rev. B **78**, 035132 (2008).

[16] S. S. Kancharla, B. Kyung, D. Sénéchal, M. Civelli, M. Capone, G. Kotliar, and A.-M. S. Tremblay, Anomalous superconductivity and its competition with antiferromagnetism in doped mott insulators, Phys. Rev. B **77**, 184516 (2008).

[17] H. Zhou, Y. Yacoby, V. Y. Butko, G. Logvenov, I. Božović, and R. Pindak, Anomalous expansion of the copper-apical-oxygen distance in superconducting cuprate bilayers, Proc. Natl. Acad. Sci. **107**, 8103 (2010).

[18] C. Weber, C. Yee, K. Haule, and G. Kotliar, Scaling of the transition temperature of hole-doped cuprate superconductors with the charge-transfer energy, Europhys. Lett. **100**, 37001 (2012).

[19] K.-S. Chen, Z. Y. Meng, S.-X. Yang, T. Pruschke, J. Moreno, and M. Jarrell, Evolution of the superconductivity dome in the two-dimensional Hubbard model, Phys. Rev. B **88**, 245110 (2013).

[20] A. T. Rømer, A. Kreisel, I. Eremin, M. A. Malakhov, T. A. Maier, P. J. Hirschfeld, and B. M. Andersen, Pairing symmetry of the one-band Hubbard model in the paramagnetic weak-coupling limit: A numerical RPA study, Phys. Rev. B **92**, 104505 (2015).

[21] Xi Chen, J. P. F. LeBlanc, and E. Gull, Superconducting fluctuations in the normal state of the two-dimensional Hubbard model, Phys. Rev. Lett. **115**, 116402 (2015).

[22] J. Vučičević, T. Ayral, and O. Parcollet, TRILEX and GW + EDMFT approach to d-wave superconductivity in the Hubbard model, Phys. Rev. B **96**, 104504 (2017).

[23] Y. Y. Peng, G. Dellea, M. Minola, M. Conni, A. Amorese, D. Di Castro, G. M. De Luca, K. Kummer, M. Salluzzo, X. Sun, X. J. Zhou, G. Balestrino, M. Le Tacon, B. Keimer, L. Braicovich, N. B. Brookes, and G. Ghiringhelli, Influence of apical oxygen on the extent of in-plane exchange interaction in cuprate superconductors, Nat. Phys. **13**, 1201 (2017).

[24] H.-C. Jiang and T. P. Devereaux, Superconductivity in the doped Hubbard model and its interplay with next-nearest hopping t', Science **365**, 1424 (2019).

[25] M. Qin, C.-M. Chung, H. Shi, E. Vitali, C. Hubig, U. Schollwöck, S. R. White, and S. Zhang (Simons Collaboration on the Many-Electron Problem), Absence of superconductivity in the pure two-dimensional Hubbard model, Phys. Rev. X **10**, 031016 (2020).

[26] C. Zhang, J.-W. Li, and J. von Delft, Frustration-induced superconductivity in the t-t' Hubbard model, arXiv:2307.14835.

[27] T. P. Devereaux, A. Virosztek, and A. Zawadowski, Charge-transfer fluctuation, d-wave superconductivity, and the B_{1g} Raman phonon in cuprates, Phys. Rev. B **51**, 505 (1995).

[28] T. P. Devereaux, T. Cuk, Z.-X. Shen, and N. Nagaosa, Anisotropic electron-phonon interaction in the cuprates, Phys. Rev. Lett. **93**, 117004 (2004).

[29] S. Johnston, F. Vernay, B. Moritz, Z.-X. Shen, N. Nagaosa, J. Zaanen, and T. P. Devereaux, Systematic study of electron-phonon coupling to oxygen modes across the cuprates, Phys. Rev. B **82**, 064513 (2010).

[30] Y. Wang, Z. Chen, T. Shi, B. Moritz, Z.-X. Shen, and T. P. Devereaux, Phonon-mediated long-range attractive interaction in one-dimensional cuprates, Phys. Rev. Lett. **127**, 197003 (2021).

[31] B. Rosenstein and B. Y. Shapiro, Apical oxygen vibrations dominant role in d-wave cuprate superconductivity and its interplay with spin fluctuations, J. Phys. Commun. **5**, 055013 (2021).

[32] Y. Fukuzumi, K. Mizuhashi, K. Takenaka, and S. Uchida, Universal superconductor-insulator transition and T_c depression in Zn-substituted high-T_c cuprates in the underdoped regime, Phys. Rev. Lett. **76**, 684 (1996).

[33] H. Eisaki, N. Kaneko, D. L. Feng, A. Damascelli, P. K. Mang, K. M. Shen, Z.-X. Shen, and M. Greven, Effect of chemical inhomogeneity in bismuth-based copper oxide superconductors, Phys. Rev. B **69**, 064512 (2004).

[34] H. Hobou, S. Ishida, K. Fujita, M. Ishikado, K. M. Kojima, H. Eisaki, and S. Uchida, Enhancement of the superconducting critical temperature in $Bi_2Sr_2CaCu_2O_{8+\delta}$ by controlling disorder outside CuO_2 planes, Phys. Rev. B **79**, 064507 (2009).

[35] S. Kim, X. Chen, W. Fitzhugh, and X. Li, Apical charge flux-modulated in-plane transport properties of cuprate superconductors, Phys. Rev. Lett. **121**, 157001 (2018).

[36] V. Stanev, C. Oses, A. G. Kusne, E. Rodriguez, J. Paglione, S. Curtarolo, and I. Takeuchi, Machine learning modeling of superconducting critical temperature, npj Comput. Mater. **4**, 1 (2018).

[37] D. Lee, D. You, D. Lee, X. Li, and S. Kim, Machine-learning-guided prediction models of critical temperature of cuprates, J. Phys. Chem. Lett. **12**, 6211 (2021).

[38] Y. Wang, T. Su, Y. Cui, X. Ma, X. Zhou, Y. Wang, S. Hu, and W. Ren, Cuprate superconducting materials above liquid nitrogen temperature from machine learning, RSC Advances **13**, 19836 (2023).

[39] P. Prelovšek and A. Ramšak, Spin-fluctuation mechanism of superconductivity in cuprates, Phys. Rev. B **72**, 012510 (2005).

[40] Y. Wang and A. Chubukov, Charge-density-wave order with momentum $(2q, 0)$ and $(0, 2q)$ within the spin-fermion model: Continuous and discrete symmetry breaking, preemptive composite order, and relation to pseudogap in hole-doped cuprates, Phys. Rev. B **90**, 035149 (2014).

[41] M. A. Metlitski and S. Sachdev, Quantum phase transitions of metals in two spatial dimensions. II. spin density wave order, Phys. Rev. B **82**, 075128 (2010).

[42] F. Onufrieva and P. Pfeuty, Superconducting pairing through the spin resonance mode in high-temperature cuprate superconductors, Phys. Rev. Lett. **102**, 207003 (2009).

[43] F. Onufrieva and P. Pfeuty, Low-doping anomalies in high-T_c cuprate superconductors as evidence of a spin-fluctuation-mediated superconducting state, Phys. Rev. Lett. **109**, 257001 (2012).

[44] S. M. O'Mahony, W. Ren, W. Chen, Y. X. Chong, X. Liu, H. Eisaki, S. Uchida, M. H. Hamidian, and J. C. Séamus Davis, On the electron pairing mechanism of copper-oxide high temperature superconductivity, Proc. Natl. Acad. Sci. **119**, 37 (2022).

[45] S. Jiang, D. J. Scalapino, and S. R. White, Ground-state phase diagram of the $t - t' - J$ model, Proc. Natl. Acad. Sci. U.S.A. **118**, e2109978118 (2021).

[46] C. Weber, T. Giamarchi, and C. M. Varma, Phase diagram of a three-orbital model for high-T_c cuprate superconductors, Phys. Rev. Lett. **112**, 117001 (2014).

[47] N. Kowalski, S. S. Dash, P. Sémon, D. Sénéchal, and A.-M. Tremblay, Oxygen hole content, charge-transfer gap, covalency, and cuprate superconductivity, Proc. Natl. Acad. Sci. USA **118**, e2106476118 (2021).

[48] D. Rybicki, M. Jurkutat, S. Reichardt, C. Kapusta, and J. Haase, Perspective on the phase diagram of cuprate high-temperature superconductors, Nat. Commun. **7**, 11413 (2016).

[49] S. Jiang, D. J. Scalapino, and S. R. White, Density matrix renormalization group based downfolding of the three-band Hubbard model: Importance of density-assisted hopping, Phys. Rev. B **108**, L161111 (2023).

[50] V. J. Emery, Theory of high-T_c superconductivity in oxides, Phys. Rev. Lett. **58**, 2794 (1987).

[51] See Supplemental Material at http://link.aps.org/supplemental/10.1103/PhysRevB.109.L081115 for detailed definitions of all quantities, derivation of the transformed Hamiltonian that we use, and a comprehensive presentation of results (including illustrative figures and tables summarizing the predictor variables that we study). The Supplemental Material also contains Refs. [18,53].

[52] N. Marzari, A. A. Mostofi, J. R. Yates, I. Souza, and D. Vanderbilt, Maximally localized wannier functions: Theory and applications, Rev. Mod. Phys. **84**, 1419 (2012).

[53] See Supplemental Material in Ref. [18].

[54] S. Lebègue, T. Björkman, M. Klintenberg, R. M. Nieminen, and O. Eriksson, Two-dimensional materials from data filtering and *ab initio* calculations, Phys. Rev. X **3**, 031002 (2013).

[55] H. C. Herper, T. Ahmed, J. M. Wills, I. Di Marco, T. Björkman, D. Iuşan, A. V. Balatsky, and O. Eriksson, Combining electronic structure and many-body theory with large databases: A method for predicting the nature of $4f$ states in Ce compounds, Phys. Rev. Mater. **1**, 033802 (2017).

[56] U. Kumar, H. W. Kim, S. Singh, S. B. Cho, and H. Ko, Designing Pr-based advanced photoluminescent materials using machine learning and density functional theory, J. Mater. Sci. **59**, 1433 (2024).

[57] K. Lejaeghere, G. Bihlmayer, T. Björkman, P. Blaha, S. Blügel, V. Blum, D. Caliste, I. E. Castelli, S. J. Clark, A. D. Corso, S. de Gironcoli, T. Deutsch, J. K. Dewhurst, I. D. Marco, C. Draxl, M. Dułak, O. Eriksson, J. A. Flores-Livas, K. F. Garrity, L. Genovese *et al.*, Reproducibility in density functional theory calculations of solids, Science **351**, aad3000 (2016).

[58] F. Aryasetiawan and F. Nilsson, *Downfolding Methods in Many-Electron Theory* (AIP Publishing LLCMelville, New York, 2022).

[59] P. Hansmann, N. Parragh, A. Toschi, G. Sangiovanni, and K. Held, Importance of d-p coulomb interaction for high T_C cuprates and other oxides, New J. Phys. **16**, 033009 (2014).